

Towards exciton-polaritons in MoS₂ nanotubes

D. R. Kazanov,* M. V. Rakhlin, K. G. Belyaev, A. V. Poshakinskiy, and T. V. Shubina
Ioffe Institute, 26 Politekhnicheskaya, St Petersburg 194021, Russian Federation

(Dated: November 10, 2021)

We measure low-temperature micro-photoluminescence spectra along a MoS₂ nanotube, which exhibit the peaks of the optical whispering gallery modes below the exciton resonance. The variation of the position and intensity of these peaks is used to quantify the change of the nanotube geometry. The width of the peaks is shown to be determined by the fluctuations of the nanotube wall thickness and propagation of the detected optical modes along the nanotube. We analyse the dependence of the energies of the optical modes on the wave vector along the nanotube axis and demonstrate the potential of the high-quality nanotubes for realization of the strong coupling between exciton and optical modes with the Rabi splitting reaching 400 meV. We show how the formation of exciton-polaritons in such structures will be manifested in the micro-photoluminescence spectra.

I. INTRODUCTION

Nanotubes (NTs) made of transition metal dichalcogenides (TMD) such as MoS₂, WSe₂, WS₂ (generalized formula is MX₂) were first synthesized in the last century [1, 2] and have been intensively investigated since then (see for review [3]). The walls of the TMD NTs consist of monolayers connected by a weak van der Waals force [4]. In the last years, the TMD structures as a whole gained increased attention due to the exceptional optical properties in the monolayer limit. In particular, the MoS₂ monolayer has the direct optical transitions in the visible range that are associated with the A-exciton which have a large oscillator strength [5, 6]. Recently, we have shown that the micro-photoluminescence (micro-PL) spectra of the multilayered MoS₂ NTs also exhibit the direct exciton emission [3]. Furthermore, the spectra are modulated by pronounced peaks linearly polarized along the tube axis, that were attributed to the optical whispering gallery modes maintained inside the NT wall [7].

The presence of both strong exciton and optical resonances opens a way to couple them when their frequencies coincide. Then, the hybrid polariton modes are formed and the interaction strength can be quantified by the Rabi splitting between them. For planar microcavities based on classical semiconductors, the Rabi splitting $\hbar\Omega_{\text{Rabi}}$ reaches the values of about 10 meV for GaAs, 20 meV for CdTe, 50 meV for GaN, and 200 meV for ZnO [8–11]. Major interest in exciton-polaritons in 2D van der Waals structures is related to the enhanced interaction between light and matter [12] as compared to classical bulk materials. In Fabry-Perot type microresonators with a single MoSe₂ monolayer, the Rabi splitting $\hbar\Omega_{\text{Rabi}} \sim 20$ meV was demonstrated. Placing N monolayers inside the cavity enhances the interaction by \sqrt{N} , and for four layers of MoSe₂ the Rabi splitting of ~ 40 meV [13] was achieved. A stronger interaction is realized for microcavities with WS₂ monolayers where the Rabi splitting reaches 270 meV for A-exciton and

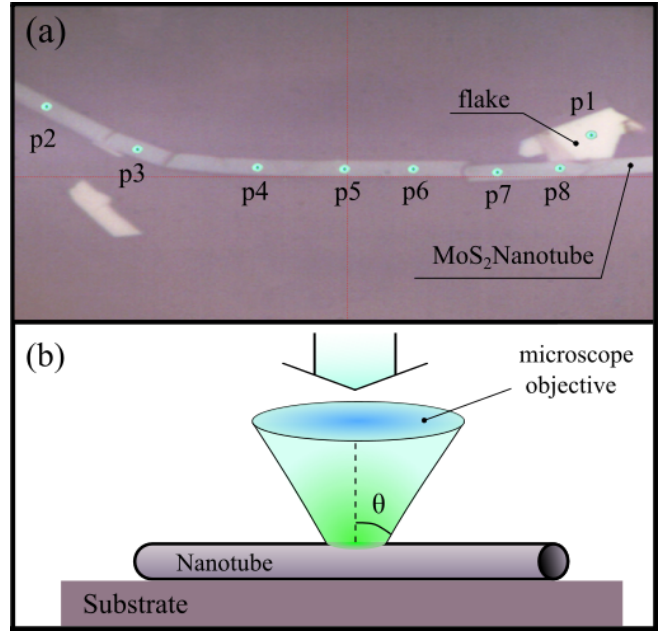


FIG. 1. (a) Image of a MoS₂ NT taken inside the micro-PL setup. The NT has few cracks that is not essential for our experiment. Green dots indicate spots where the micro-PL was measured. (b) Schematic of NT excitation at micro-PL measurement (not to scale). As shown, the lens collects the emission at angles $\theta \lesssim 25^\circ$.

780 meV for B-exciton [14] at low temperatures and is about 70 meV [15] at room temperature. Geometry more complex than the planar allows for fine tuning of polariton spectra. The interaction of excitons with the waveguide mode in the structures based on MoSe₂ was demonstrated to produce the Rabi splitting of ~ 100 meV [16]. Possible Rabi splitting of about 280 meV was derived via analysis of extinction spectra of an ensemble of WS₂ nanotubes [17].

In this paper, we investigate micro-PL of MoS₂ NTs. We model the micro-PL spectra and reproduce the peaks associated with whispering gallery modes. Our studies reveal that the position of peaks fluctuates along the NT due to the variation of the wall width, whereas the broad-

* kazanovdr@gmail.com

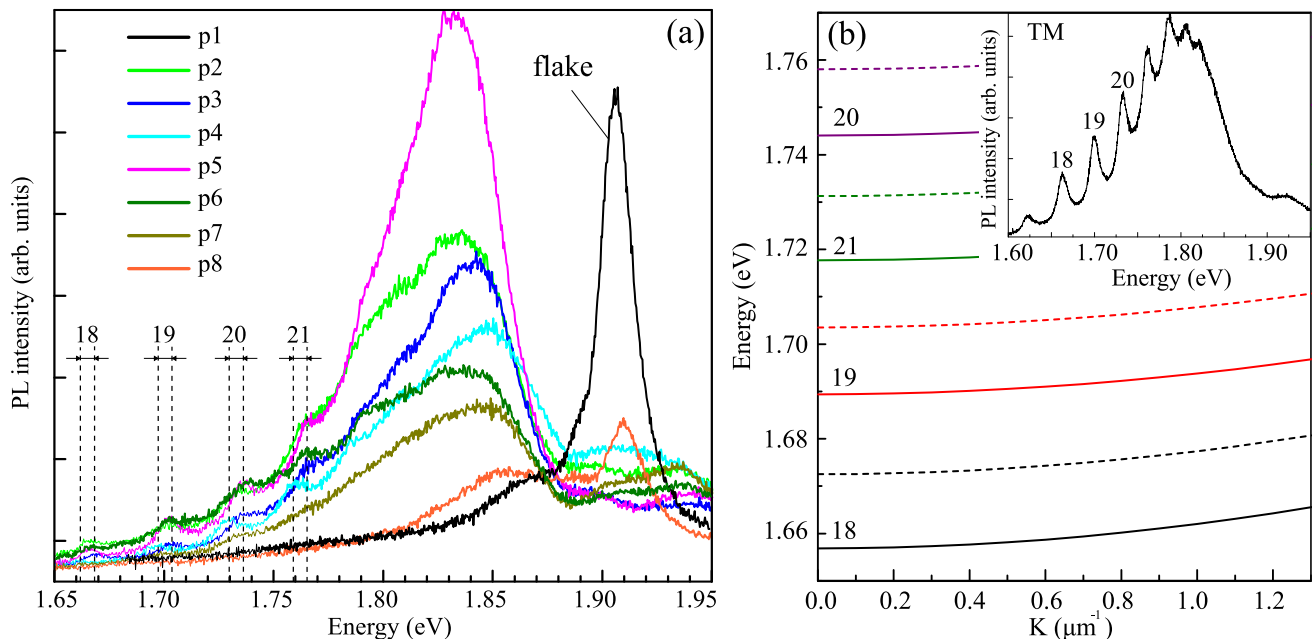


FIG. 2. (a) Non-polarized micro-PL spectra measured at 10 K in the spectral range of direct exciton transitions from several spots of MoS₂ NT, indicated by green dots in Fig. 1a. Black line is a spectrum taken from the planar MoS₂ layer (p1, flake). The dotted lines indicate the energies of the TM-polarized whispering gallery modes with angular quantum numbers $m = 18 - 21$ calculated for the NT with the wall thickness varying by 1 monolayer. (b) Dependence of the energies of the optical modes with the angular numbers $m = 18 - 21$ on the wave vector K along the NT axis calculated for NTs with the 44-monolayers wall (dashed lines) and 46-monolayers wall (solid lines). The inset shows the TM-polarized micro-PL spectrum of the NT at 80 K when the intensity of basic exciton peak quenches.

ening of the peaks is determined by the dispersion of the optical modes, whose impact occurs via the finite numerical aperture of used objective. We propose to use NTs of high quality as a microresonator to realize the strong coupling between the optical modes and excitons and show how formation of the exciton-polaritons would transform the PL spectra.

II. EXPERIMENT AND MODELING OF OPTICAL MODES

To study the optical properties of single MoS₂ NTs, a micro-PL experiment was performed. A sample with NTs on a Si substrate [7] was mounted in a He-flow cryostat with an Attocube XYZ piezo-driver inside, which allowed to precisely maintain the positioning of a chosen part on a NT with respect to a laser spot. Micro-PL measurements were performed at low temperature of 10 K, when the direct exciton emission prevails [3]. Focusing of a laser beam on the sample was carried out using a 50-fold objective (Mitutoyo 50xNIR, NA = 0.42), which also was used to collect the PL signal. The enlarged image of the sample was transferred by means of achromatic lens to the plane of a mirror with a calibrated aperture (pinhole - 200 μm). This arrangement determined the region on the sample from which the micro-PL signal is detected. To record the PL spectra from the NT the collected sig-

nal passed through the gratings of the monochromator and entered the CCD camera. A 405-nm line of a semiconductor laser was used for non-polarized PL excitation. The laser power density correspond to ~ 10 mW per area of about 20–50 μm^2 .

Figure 1a shows a photo of a NT taken inside of the micro-PL setup. The NT is about 50 microns in length and 2 microns in diameter. The green dots p1–p8 show the locations from which the micro-PL signal was recorded. Their size corresponds approximately to the size of the signal detection spot in the experiment. The number of layers in the NT wall has been determined by modeling the micro-PL spectra, as described in Ref. [7], which yields the average value of about 45 monolayers.

The micro-PL spectra in the optical range of the direct exciton transitions measured in different spots of the NT are shown in Fig. 2a. The black line indicates the spectrum taken from the surface of the plane layer (flake) featuring a bright inhomogeneously broadened exciton resonant peak. The major peaks in the micro-PL spectra recorded from NT are wider and red shifted by ~ 50 meV with respect to the flake due to uncompensated stresses and 3R-polytype stacking of the monolayers in the wall of the chiral NT [3, 18]. While the peaks at about ~ 1.83 eV correspond to A-exciton in MoS₂, the series of smaller peaks at lower energies stems from TM-polarized optical whispering gallery modes in the NT. Here, they are characterized by angular quantum num-

ber $m = 18$ – 21 . Modes with energies higher than the exciton energy are not observed due to the strong absorption. TE-polarized whispering gallery modes are absent in the spectrum due to their lower Q -factor that makes them much less pronounced. The black dashed lines in Fig. 2a indicate the maximum deviation in the positions of the peaks detected from different spot of the NT. For all of the observed modes, the spread is around 6 meV, which corresponds to a change of the wall thickness by 1 monolayer.

The intensity of the PL is maximal in the center of the NT, point p5 in Fig. 1a, and decreases at the NT end. Analyzing the evolution of the spectra from point p5 to point p8 in Fig. 2a, we can assume that the geometry of the NT is adiabatically changing as it becomes less like a NT and more like a ribbon (flattened tube). This is also confirmed by a decrease in the intensity of the peaks associated with the presence of optical modes and an increase in the intensity of the peak associated with the flat layer. It should be noted that NTs start to form inside microfolds or bend edges of curved flakes [2]. To put a NT on the SiO₂ substrate one should tear it from the silica ampoules where the NTs were grown. The point p8 corresponds to the tip of the NT, which consists of a chunk of the flake and the incipient part of the NT. Thus, due to the limited spatial resolution, we observe PL contributions from both the NT and the flake which has approximately the same thickness. The other end of the tube (points p2–p4) turns out to be undamaged, as we observe pronounced optical modes in the corresponding spectra. In addition, we have shown TM-polarized micro-PL spectrum where the peaks corresponding to whispering gallery modes are more pronounced (see the inset in Fig. 2b).

To model the PL spectra, we solve Maxwell's equations for the hollow cylinder with a certain inner and outer radii, dielectric permittivity of MoS₂, and the homogeneously distributed sources of radiation. Generalizing the approach developed in [7], we calculate the radiation intensity not only in the direction perpendicular to the NT axis, but also in other directions, characterized by angle θ , see Fig. 1b. In the experiment, the PL from the directions with $\theta \lesssim 25^\circ$ is collected by the microscope objective. Therefore, the PL spectra is contributed by the optical modes of frequency ω corresponding wave vector along the tube axis $K = (\omega/c) \sin \theta \lesssim 3.5 \mu\text{m}^{-1}$ (c is the speed of light). The spread of their energies widens the PL peaks.

Figure 2b shows the dependence of the energies of the optical modes with angular numbers $m = 18 - 21$ on the wave vector along the NT axis K . Calculation was made for NTs with the wall consisting of 44 (dashed lines) and 46 monolayers (solid lines). Reduction of the NT wall thickness leads to the increase of the mode energies due to the stronger confinement. The dependence of the mode energies on the wave vector K can be expressed as $E(K) = \hbar c / n_{\text{eff}} \sqrt{K^2 + (m/R)^2}$, where R is the NT radius, n_{eff} is the effective refractive index, which can be

estimated as $n_{\text{eff}} \approx n\eta$ with $\eta \approx 0.44$ being the part of the electric field that is confined inside the NT wall. For small wave vectors $K \ll m/R$ considered here, the dispersion is quadratic, $E(K) = E(0) + \hbar^2 K^2 / 2M^*$, with the effective mass $M^* = \hbar m n_{\text{eff}} / (Rc) \approx 7.7 \cdot 10^{-6} m_0$, where m_0 is the mass of the free electron. Numerically calculated dispersion shown in Fig. 2d yields the close value $M^* = 7.4 \cdot 10^{-6} m_0$. Then, the PL peak broadening due to finite spread of detection angles is estimated as $\delta E \approx E^2 \sin^2 \theta / (2M^* c^2) = 55$ meV. This value shows the upper bound of the peak width observed in the experiment. To sum up all of the above, PL spectra indicate that the actual tube of MoS₂ is not homogeneous. The observed variation of the peak positions in the PL spectra from different parts of the NT is due to the fluctuations of the NT wall thickness. The PL peak width is additionally contributed by the finite PL detection angle.

III. POLARITONS IN NANOTUBE RESONATOR

In the above considerations, the exciton resonance was assumed to have strong inhomogeneous broadening. Qualitatively new effects are expected in the higher-quality structures with sharp exciton resonances where the strong coupling regime between the optical modes of the NT and the excitons can be realized. The important role is played by the wave vector along the NT axis K that allows for the fine tuning of the optical mode energy to match the exciton energy. Here, we discuss the properties of such hybrid exciton-polariton modes in such case and show how they would be manifested in the PL spectra.

To calculate the dispersion of exciton-polaritons in the NT resonator, we assume that its walls are characterized by the local single-pole dielectric function

$$\varepsilon(\omega) = \varepsilon_b \left(1 + \frac{\omega_{\text{LT}}}{\omega_{\text{ext}} - \omega - i\Gamma} \right), \quad (1)$$

where ω_{LT} is a longitudinal-transverse splitting, ω_{ext} is the exciton peak frequency. We estimate its value from the known radiative exciton life time of $1/(2\Gamma_0) = 0.23$ ps in the MoS₂ monolayers [19]. Assuming that the NT wall consists of dozens of isolated monolayers (the certain isolation can be supposed for the strained chiral tubes), the longitudinal-transverse splitting is calculated as [20]

$$\omega_{\text{LT}} = \frac{2\Gamma_0 c}{\omega_{\text{exc}} d \sqrt{\varepsilon_b}}, \quad (2)$$

where $\varepsilon_b = 16.2$ is the background dielectric constant of MoS₂ and $d = 6.7 \text{ \AA}$ is the interlayer distance, yielding $\hbar\omega_{\text{LT}} \sim 114$ meV. The strength of the interaction of optical mode and exciton can be quantified by the value of the Rabi splitting between the energies of the hybrid polariton modes, which are formed when the energies of bare excitations coincide.

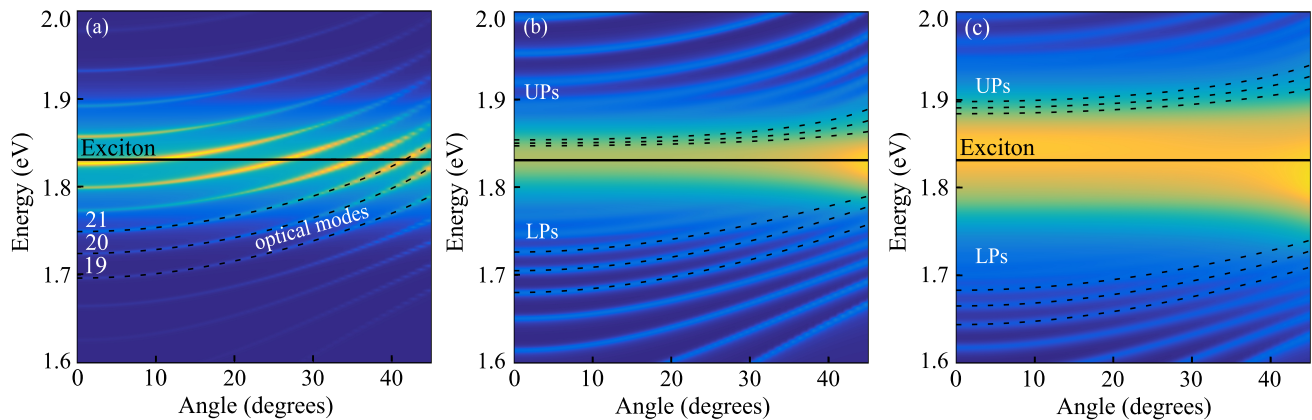


FIG. 3. Color plot of the PL spectra dependence on the detection angle calculated for the NTs without inhomogeneous broadening of the exciton resonance and different values of Rabi splitting, 2 meV, 20 meV, and 200 meV (from left to right). The dotted lines show the dispersion of the eigenmodes with the angular quantum numbers $m = 19, 20, 21$. The black solid line indicates the energy of the exciton. UPs and LPs denote upper and lower polariton modes, respectively.

The interaction value under the conditions of the exact resonance of the exciton energy $E_{\text{exc}}(K)$ and the optical mode mode $E_m(K)$ is denoted by the Rabi splitting $\hbar\Omega_{\text{Rabi}}$. Taking into account that only the fraction $\eta \approx 0.44$ of the optical mode has the electric field inside the NT wall and can interact with excitons (see Ref. 21 for a similar consideration for polaritons in cylindrical cavities), the Rabi frequency is calculated as

$$\Omega_{\text{Rabi}} = \sqrt{2\omega_{\text{ext}}\omega_{\text{LT}}\eta}, \quad (3)$$

which yields $\hbar\Omega_{\text{Rabi}} \sim 400$ meV. The Rabi splitting in the considered structure surpasses the typical values for the resonator structures based on classical semiconductors such as GaAs or GaN. This highlights the potential of the high-quality NT resonators based on MoS₂ for realization of strong light-exciton interaction. In the state-of-the-art structures the potentially large Rabi splitting turns out to be masked by even stronger inhomogeneous broadening.

To show the effect of strong light-exciton interaction, we calculate the PL spectra as a function of detection angle for different value of the Rabi splitting, see Fig. 3. In the regime of weak interaction, see panel (a) corresponding to $\hbar\Omega_{\text{Rabi}} = 2$ meV, the PL spectra consists of the peaks corresponding to the optical modes with different angular numbers m . The intensity of the peaks grows when they approach exciton resonance energy, but their energies (dashed lines) remain unperturbed. The increase of the light-exciton interaction strength leads to appearance of a series of anti-crossings, each of them reflecting the interaction of an optical mode and the excitonic mode with the same angular quantum number m , see panels (b) and (c) corresponding to $\hbar\Omega_{\text{Rabi}} = 20$ and 200 meV. The modes with different m , which were degenerate in the absence of interaction, are now split into

upper and lower polariton modes and a broad peak at the exciton frequency appears between them.

IV. SUMMARY

In this work, we have studied the micro-PL from the MoS₂ NTs. The spectra of micro-PL from different parts of the NT, as well as from the planar layer MoS₂ (flake) were compared. In addition to the main peak associated with the optical A-exciton transition, the peaks corresponding to the whispering gallery modes, dominating in TM polarization, were observed. Variation of the PL spectra measured from different parts of the NT indicates the change of the NT geometry from the cylindrical tube to collapsed ribbon-like one. We also observed a shift of the energies of the optical modes due to the variation of the number of monolayer in the NT wall. The peaks are additionally broadened due to the dependence of the optical mode energies on the wave vector along the NT axis and the finite spread of the PL detection angles. We have predicted the high potential of high-quality NT with low inhomogeneous broadening for realization strong coupling between light and excitons. We have calculated the PL spectra of such structures and discussed the signatures that will allow for experimental identification of exciton-polaritons in NTs, once the quality of the structures is improved.

ACKNOWLEDGEMENT

The work was supported by the Russian Science Foundation (project # 19-12-00273). A. V. P. acknowledges the partial support from RFBR grant No. 18-32-00486, the Russian President Grant No. MK-599.2019.2, and the Foundation ‘‘BASIS’’. The authors thank M. Remškar and S. Fathipour for providing the samples.

-
- [1] R. Tenne, L. Margulis, M. Genut, and G. Hodes, Polyhedral and cylindrical structures of tungsten disulphide, *Nature* **360**, 444 (1992).
- [2] M. Remškar, Z. Skraba, F. Cléton, R. Sanjinés, and F. Lévy, MoS₂ as microtubes, *Appl. Phys. Lett.* **69**, 351 (1996).
- [3] T. V. Shubina, M. Remškar, V. Yu. Davydov, K. G. Belyaev, A. A. Toropov, and B. Gil, Excitonic emission in van-der-Waals nanotubes of transition metal dichalcogenides. Review, *Annalen der Physik*, 1800415 (2019).
- [4] C. N. R. Rao and M. Nath, Inorganic nanotubes, *Dalton Trans.* **1**, 1-24 (2003).
- [5] A. Arora, M. Koperski, K. Nogajewski, J. Marcus, C. Faugeras, and M. Potemski, Excitonic resonances in thin films of WSe₂: from monolayer to bulk material, *Nanoscale* **7**, 10421 (2015).
- [6] C. Robert, M. A. Semina, F. Cadiz, M. Manca, E. Courtade, T. Taniguchi, K. Watanabe, H. Cai, S. Tongay, B. Lassagne, P. Renucci, T. Amand, X. Marie, M. M. Glazov, and B. Urbaszek, Optical spectroscopy of excited exciton states in MoS₂ monolayers in van der Waals heterostructures, *Phys. Rev. Materials* **2**, 011001 (2018).
- [7] D. R. Kazanov, A. V. Poshakinskiy, V. Yu. Davydov, A. N. Smirnov, I. A. Elisseyev, D. A. Kirilenko, M. Remškar, S. Fathipour, A. Mintairov, A. Seabaugh, B. Gil, and T. V. Shubina, Multiwall MoS₂ tubes as optical resonators, *Appl. Phys. Lett.* **113**, 101106 (2018).
- [8] E. Wertz, L. Ferrier, D. D. Solnyshkov, R. Johne, D. Sanvitto, A. Lemaitre, I. Sagnes, R. Grousson, A. V. Kavokin, P. Senellart, G. Malpuech, and J. Bloch, Spontaneous formation and optical manipulation of extended polariton condensates, *Nature Phys.* **6**, 860 (2010).
- [9] J. Kasprzak, M. Richard, S. Kundermann, A. Baas, P. Jeambrun, J. M. J. Keeling, F. M. Marchetti, M. H. Szymanska, R. Andre, J. L. Staehli, V. Savona, P. B. Littlewood, B. Deveaud, and L. S. Dang, Bose-Einstein condensation of exciton polaritons, *Nature* **443**, 409 (2006).
- [10] G. Christmann, R. Butte, E. Feltn, A. Mouti, P. A. Stadelmann, A. Castiglia, J.-F. Carlin, and N. Grandjean, Large vacuum Rabi splitting in a multiple quantum well GaN-based microcavity in the strong-coupling regime, *Phys. Rev. B* **77**, 085310 (2008).
- [11] F. Li, L. Orosz, O. Kamoun, S. Bouchoule, C. Brimont, P. Disseix, T. Guillet, X. Lafosse, M. Leroux, J. Leymarie, M. Mexis, M. Mihailovic, G. Patriarche, F. Reveret, D. Solnyshkov, J. Zuniga-Perez, and G. Malpuech, From excitonic to photonic polariton condensate in a ZnO-based microcavity, *Phys. Rev. Lett.* **110**, 196406 (2013).
- [12] T. Low, A. Chaves, J. D. Caldwell, A. Kumar, N. X. Fang, P. Avouris, T. F. Heinz, F. Guinea, L. Martin-Moreno, and F. Koppens, Polaritons in layered two-dimensional materials, *Nature Materials* **16**, 4792 (2016).
- [13] S. Dufferwiel, S. Schwarz, F. Withers, A. A. P. Trichet, F. Li, M. Sich, O. Del Pozo-Zamudio, C. Clark, A. Natilov, D. D. Solnyshkov, G. Malpuech, K. S. Novoselov, J. M. Smith, M. S. Skolnick, D. N. Krizhanovskii, and A. I. Tartakovskii, Exciton-polariton in van der Waals heterostructures embedded in tunable microcavities, *Nat. Comm.* **6**, 8579 (2015).
- [14] Q. Wang, L. Sun, B. Zhang, C. Chen, X. Shen, and W. Lu, Direct observation of strong light-exciton coupling in thin WS₂ PLakes, *Optics Express* **24**, 007151 (2016).
- [15] L. C. Platten, Z. He, D. M. Coles, A. A. P. Trichet, A. W. Powell, R. A. Taylor, J. H. Warner, and J. M. Smith, Room-temperature exciton-polaritons with two-dimensional WS₂, *Sci. Rep.* **6**, 33134 (2016).
- [16] F. Hu, Y. Luan, M. E. Scott, J. Yan, D. G. Madruga, X. Xu, and Z. Fei, Imaging exciton-polariton transport in MoSe₂ waveguides, *Nature Photonics* **11**, 356 (2017).
- [17] L. Yadgarov, B. Visic, T. Abir, R. Tenne, A. Yu. Polyakov, R. Levi, T. V. Dolgova, V. V. Zubyuk, A. A. Fedyanin, E. A. Goodilin, T. Ellenbogen, R. Tenne, and D. Oron, Strong light-matter interaction in tungsten disulfide nanotubes, *Phys. Chem. Chem. Phys.*, **20**, 20812 (2018).
- [18] J. A. Wilson and A. D. Yoffe, The transition metal dichalcogenides discussion and interpretation of the observed optical, electrical and structural properties, *Adv. Phys.* **18**, 193 (1969).
- [19] M. Palumbo, M. Bernardi, and J. C. Grossman, ex, *Nano Lett.* **15**, 2794 (2015).
- [20] E. L. Ivchenko, Optical spectroscopy of semiconductor nanostructures, Alpha Science International, Harrow, U.K. (2005).
- [21] M. A. Kaliteevski, S. Brand, R. A. Abram, A. Kavokin, and L. S. Dang, Whispering gallery polaritons in cylindrical cavities, *Phys. Rev. B* **75**, 233309 (2007).